Engineering Structures 21 (1999) 877–882

ENGINEERING STRUCTURES

Seismic study of an historic covered bridge

Constantine C. Spyrakos [a,b,*], Emory L. Kemp [a], Ramesh Venkatareddy [a]

[a] West Virginia University, Morgantown WV 26506-6103, USA
[b] National Technical University of Athens, Zografos, 15700, Athens, Greece

Received 25 January 1996; received in revised form 14 February 1997; accepted 23 April 1997

Abstract

The covered timber bridge has become an icon of the nation's bucolic nineteenth-century past. The public reveres these quaint structures without really understanding their historic significance, either as a visible sign of the internal improvements movement (a dominant theme in the early years of the Republic) nor of their pioneering role in the development of American truss bridges. One of these survivors is the (West Virginia) Barrackville Bridge, completed to the patented Burr arch-truss design in 1853 by West Virginia's pioneering covered bridge builder, Lemuel Chenoweth. As part of a comprehensive restoration program expected to be completed in 1998, this paper describes the expected static and seismic behavior of the restored bridge. These analyses were performed using current AASHTO, nineteenth-century loading conditions, for code specific and historic earthquakes. The results serve as a basis of the restoration design. © 1999 Elsevier Science Ltd. All rights reserved.

Keywords: Timber bridges; Historic bridges; Analytical/experimental studies; Seismic analysis

1. Background

In the nineteenth century, numerous timber covered bridges were erected in the Virginias as part of a network of turnpike roads. Apparently, at least 400 were built at one time or another in West Virginia, but now only 17 remain. In the neighboring state of Pennsylvania, where 4,000 bridges were built at one time or another, only 220 survive. In Ohio, where a multitude of bridges were built, only 129 are extant, and there are numerous other survivors in Indiana, New England, and elsewhere. Nevertheless, they are a vanishing breed succumbing at a rapid rate to flood, fire, vandalism and neglect.

A pair of outstanding ante-bellum arch-truss bridges remain in West Virginia, the handiwork of Lemuel Chenoweth and his brother, Eli. Both the recently restored Philippi Covered Bridge (built in 1852) and the Barrackville Bridge (finished a year later) are testimonies to the Chenoweth brothers. The Barrackville Bridge spans the Buffalo Creek near Fairmont, West Virginia in the village of Barrackville, on the Fairmont to Wheeling Turnpike. The site also includes part of the original alignment of the Baltimore and Ohio Railroad, America's first "trunk line railway." The Barrackville bridge played a role in the Civil War when the Jones–Imboden Raiders appeared at the bridge site on their way to Morgantown in 1862. The Philippi Bridge also played a role in the Civil War, and these two survivors are the most historically significant covered bridges in West Virginia.

The study of the Barrackville Bridge and its response in resisting static and seismic loads is the main objective of this paper. To the authors knowledge, this is the first published comprehensive study of a covered bridge that includes seismic analysis. The results of this study have been integrated into a basic restoration plan to ensure the safety of the bridge while preserving as much of the original fabric as possible.

2. Barrackville Bridge restoration

An earlier analysis of the Barrackville Bridge to determine the characteristics of the combined kingpost truss and arch revealed that the arch was considered as a stiffening member, and validated the old "rule of thumb" that when wooden spans exceeded 100 feet an arch was recommended. In addition to stiffening the bridge, the arch adds considerable strength to the structure.

* Corresponding author. Tel.: + 30-1-7721187; Fax: + 30-1-7721182; E-mail: chris@central.ntua.gr

PII: S0141-0296(98)00041-8

On the basis of this study and experience gained in the 1991 restoration of the Philippi Bridge, the restoration methodology utilized was driven by static structural analysis. Each member or joint was analyzed and compared to the required capacity. The rule was to repair whenever possible rather than replace.

Since the soundness of each joint could not be determined by visual inspection, a series of non-destructive tests were undertaken to determine the extent, if any, of the rot in the joints. Non-destructive testing data established which joints are to be repaired according to details included in the contract documents. The bridge is to be restored (for pedestrian use only) to a period shortly after the Civil War, ca. 1870, when it was first enclosed with a roof and siding. As a result, both the static and seismic analyses were based on the restored structure with sound members and joints.

The span of the bridge is 40.28 m measured from center-to-center of the supports and the width is 5.0 m. The structural system consists of two main multiple-kingpost trusses each flanked by a pair of arches (see Fig. 1). The floor is resting on the bottom chord of the truss. The original road surface of 5 cm × 10 cm timber planks was laid 45 degrees to the flow of the traffic and is supported by stringers also laid at 45 degrees and 90 degrees to the deck planks. The stringers were then carried by transverse floor beams at the panel points.

The roof truss is made up of a series of transverse members reaching from the vertical posts of one side truss to the other. Between each of these members is a cross bracing secured by wooden pegs and wedges. The same use of pegs (i.e. treenails) were used in the joints, whereas wood joggles secured with wrought-iron bolts were employed for splices in the bottom chord. A detailed description is given by Kemp and Hall [1], while Cohen [2] provides data on all of West Virginia's covered bridges.

The end vertical posts of the truss and the ends of arch meet at the abutment. The abutments are built of approximately 92 cm × 92 cm stone blocks fitted together without any bonding material. Flood rods were provided to hold the timber work to the abutments in case of excessively high flood levels.

3. Static analysis

Linear static analysis of the restored bridge was performed for two different types of loading: live loading to simulate 19th century loading, and modern truck loading as specified in AASHTO [3]. The 19th century loading assigns uniform dead load of 13200 N/m, and a uniform live load of 4130 N/m. The AASHTO lane loading specifies a uniform live load of 9300 N/m, plus a concentrated load of 80 KN for moment or 120 KN for shear, placed wherever the stresses become critical when added to the dead load of 13200 N/m. All members and joints were assumed to be repaired and fully functional for both the static and seismic analyses.

4. Seismic analysis

According to AASHTO, a detailed seismic analysis is not required for simple span bridges. However, because of the historic significance of the Barrackville Bridge a multimode spectral analysis was applied to obtain the bridge response to four different spectra. The first spectrum was developed according to the current AASHTO specifications, while the second and third spectra were based on historic earthquakes of the region. For the region of the bridge site in West Virginia, the code [3] assigns a horizontal acceleration coefficient, *A*, of 0.05. The ground acceleration specified by the AASHTO cor-

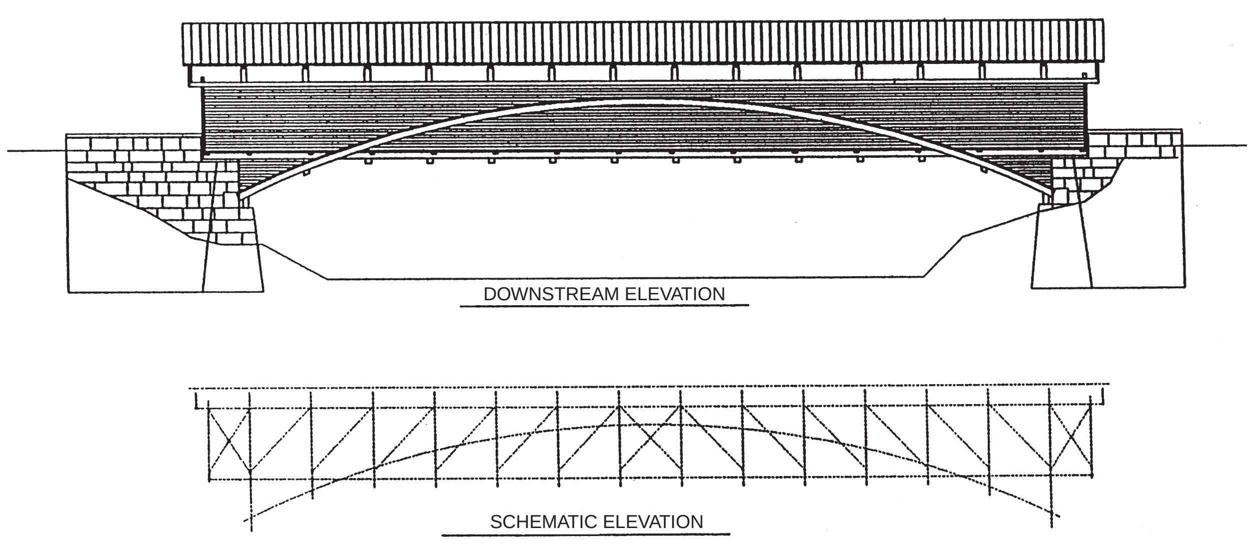

Fig. 1. Barrackville Bridge.

responds to a 10% probability of being exceeded in 50 years. Because of the historic significance of the bridge, the A value was increased to 0.06 to correspond to a 10% probability of being exceeded in 100 years [4]. A recent study on the seismic hazard of West Virginia (by King et al. [5]) has indicated intensities in several parts of the state three units higher in the MMI scale than what was previously mapped. Several regions in southern and northern West Virginia have experienced at least two seismic motions of intensity level greater than VI (MMI). In addition several of these areas, as well as the bridge site, are underlain by unlithified clay deposits which could amplify seismic excitations. Based on historic data, a modified Mercalli scale VII seismic motion has been used as basis to develop additional spectra. These spectra can be characterized with an $0.15 < A < 0.25$ (TMS-809-10-1) [4]. In this study acceleration coefficients of 0.19 and 0.25 were selected. Because of its historic significance, the bridge was assigned an importance classification factor I. Based on the AASHTO specifications [3] the bridge should be characterized as seismic performance category SPC = A for the small acceleration coefficient, and as SPC = B for $A = 0.19$, and SPC = C for $A = 0.25$. The spectra were developed for the site coefficient $S = 1.2$. An additional modification was applied to the elastic seismic response coefficient, C_{sm}. Specifically, since the AASHTO code C_{sm} is based on a 5% critical damping, it was reduced by 10% to correspond to a 7% of critical damping [4]. The higher value of damping characterizes timber structures more realistically. Seismic analysis was also performed for $A = 0.35$ to examine the response of this bridge as representative of the many historic timber bridges built in the US in areas with stronger historic earthquakes than the Barrackville Bridge site.

The design loads were obtained by superimposing the dead loads to the elastic seismic forces applied along the longitudinal and transverse directions of the bridge according to AASHTO [3]. It should be noted that the response modification factor $R = 1$ was assigned to the superstructure. Because of insufficient data about the soil conditions, the behavior of the abutments was not studied.

5. Structural modeling and results

Because of the high degree of indeterminacy of the arch-truss system, a finite element analysis was employed to study the response of the structure (see Fig. 2). The bridge is modeled with three-dimensional beam elements conforming to the guidelines given in Spyrakos [6]. End-moment releases were specified at diagonal and vertical elements to simulate pinned joints to the top and bottom chords. A typical arch-vertical/lower-chord intersection is shown in Fig. 3. Moments are also released on the arches at the abutments. The dynamic analysis was based on a lumped mass formulation [6]. The following assumptions were made:

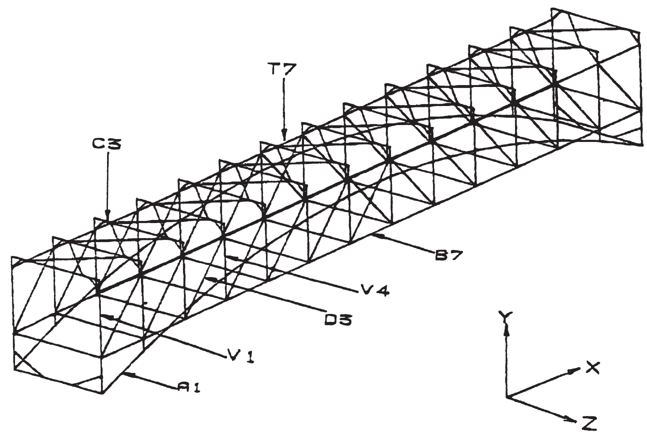

Fig. 2. 3-D FEM model of bridge.

1. The arch is pinned to verticals, diagonals and the lower chord.
2. The loads and reactions are applied only at joints.
3. Besides the lumped masses generated at the nodes to simulate the inertia of members, additional lumped masses are introduced at the bottom chords to simulate the inertia of the deck, and at nodes of the upper chord to account for the inertia of the bridge cover.

The material properties for clear yellow poplar used for structural members were obtained from in-situ ultrasonic tests performed by Halabe et al. [7] It was selected from several nondestructive techniques such as acoustic emission and modal testing. In acoustic emission testing, the detected energy is released from within the test object rather than an external source [8] as elaborated by Halabe [9]. In general, the method is limited to areas with low acoustical noise. Modal testing requires accurate evaluation of higher modes in order to assess damage, a process which is rather difficult to perform with in-situ testing [10]. Ultrasonic inspection is superior in penetrating power and high sensitivity for detection of flaws deep inside the specimen, even for extremely small flaws. Ultrasonic field testing was performed on wooden joints of the Barrackville Bridge in the summer of 1993 to assess their integrity. Tests revealed that members were severely damaged at the joints of the lower-chords [9]. A few members were also found to be structurally weak based on visual inspection. Members with velocities under 1450 m/sec, about one standard deviation below the average, were classified as weak. The results showed that about 50% of the joints were structurally deficient [9]. As documented in [9] the portable electronic instrumentation used for the in-situ testing of the Barrackville Bridge has greater accuracy compared to other non-destructive instrumentation in evaluating stiff-

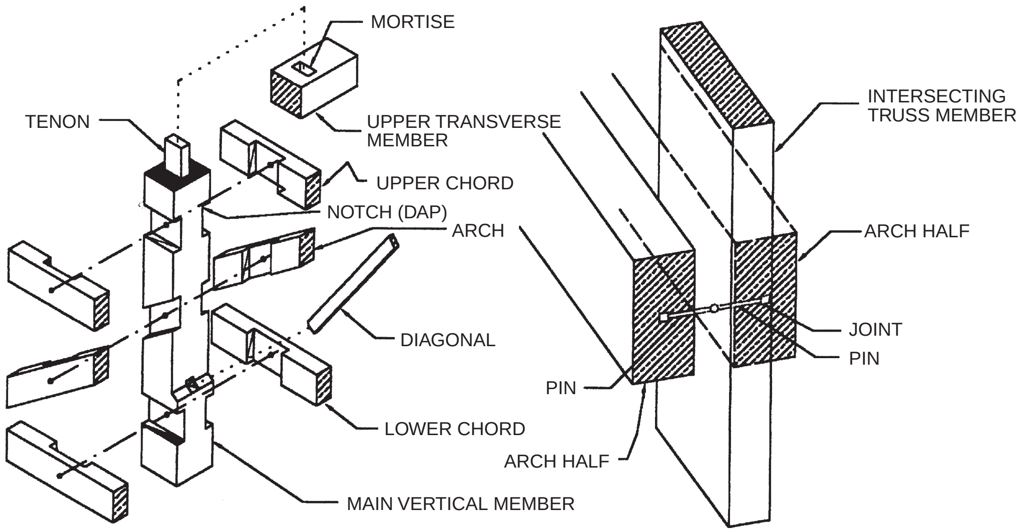

Fig. 3. Intersection of arch-vertical and lower chord (Kemp and Hall, [1]).

ness, strength properties, and detection of rot and knots in wood.

In-situ testing measured that the modulus of elasticity of timber was 8.4×10^6 kN/m^2. A unit mass of 590 kg/m^3 for timber is used in the analysis. The allowable stresses for seasoned yellow poplar under compression and tension parallel to the grain are 11,870 kN/m^2 and 13,800 kN/m^2, respectively [11]. The allowable shear stress parallel to the grain is 1,100 kN/m^2.

For static loads the resultant of dead and live load stresses at selected members: top chord (T7), diagonal (D3), vertical (V4), arch (A1) and bottom chord (B7), top cross beam (C3), and vertical (V1) are shown in the Table 1, and the sizes of selected members are shown in Table 2. The negative sign indicates compressive axial load. Notice that the maximum stresses in the members caused by dead load plus live load are nearly one-third of the allowable stresses. A unique behavior of the stress variation in the bottom chord, diagonals, and vertical members has been observed. Usually, in a kingpost truss system the magnitude of stress increases towards mid-span. However, in the Barrackville Bridge the pattern is observed only in the central seven members of the lower-chord. It should be pointed out that members in the bottom chord are in compression, while several diagonal and vertical members, normally under compression, are under tension. In the arch the compressive stresses increase away from the mid-span towards the supports. Also the high stresses in the arch indicate that the arch carries a significant part of the load, e.g., member A1. Basically the arch acts like a stiffener in the multiple-kingpost truss that reduces deflections. Even the top

Table 2
Member sizes

Member	Size in (m^2)
T7	0.0987
D3	0.0309
V4	0.0779
A1	0.1824
B7	0.0929
C3	0.0374
V1	0.0813

Table 1
Static analysis results

Loading Member	2-D 19th century Max. stress (kN/m^2)	AASHTO truck Max. stress (kN/m^2)	3-D 19th century Max. stress (kN/m^2)	AASHTO truck Max. stress (kN/m^2)
T7	−1868.5	−3924.7	−1791.9	−3803.3
D3	−2598.5	−5032.2	−2592.3	−5043.2
V4	1480.7	2926.9	1472.4	2933.2
A1	−2726.8	−5162.6	−2708.2	−5141.9
B7	364.6	1155.0	362.9	1155.0
C3	−528.5	−984.1	−535.1	−983.2
V1	−675.3	−1242.1	−675.1	−1235.8

Table 3
Static deflections

	Due to dead load, in (mm)		Due to live load, in (mm)		Total, in (mm)	
Arch truss loading	2-D	3-D	2-D	3-D	2-D	3-D
19th century loading	10.87	10.54	3.53	3.50	14.40	14.04
AASHTO truck loading	10.87	10.54	18.36	18.21	29.23	28.75

cross beams share a considerable amount of load, e.g., member C3. Table 3 lists the deflections at mid-span that would be caused by 19th century [1] and AASHTO [3] loadings. For comparison purposes the analysis has been performed twice, once using a two-dimensional (2-D), and also using a three-dimensional model (3-D). The three-dimensional model used for static, modal and seismic analysis is shown in Fig. 2. As indicated in Table 3 the deflections obtained by both models are practically identical for the static loads.

The shear stresses parallel and perpendicular to the grain applying AASHTO lane load were also examined. In all cases the results showed that the factor of safety was close to 2.5. It seems that the geometry and sizes of the members are well suited for the arch-truss action. None of the members was over-stressed under either 19th-century or AASHTO loadings.

The lowest six natural frequencies and periods of a 3-D modal analysis of the system are listed in Table 4. Also listed is the relationship between the deformation magnitudes of the corresponding mode shapes. Fig. 4 shows the lower-two mode shapes in two different plan views. As expected, the predominant deformation exhibited by the first mode is along the transverse direction. Notice that both modes are characterized by both flexural and torsional deformations about the Y and X axes, respectively. The torsional deformations are primarily introduced by the differences in inertia distribution and stiffness between the top cross bracings with the roof and the floor beams with the deck, see Fig. 2.

The most severe action of seismic load is a combination of a 100% in the transverse and 30% in the longitudinal direction [3]. The displacements at the center node of the lower cord caused by dead and seismic loads for $A = 0.25$ are given in Table 5. Table 6 lists the stresses parallel to the grain under dead load, seismic load as well as the combined stress for $A = 0.25$ at representative members which include the most heavily loaded members. Demand stresses were compared with

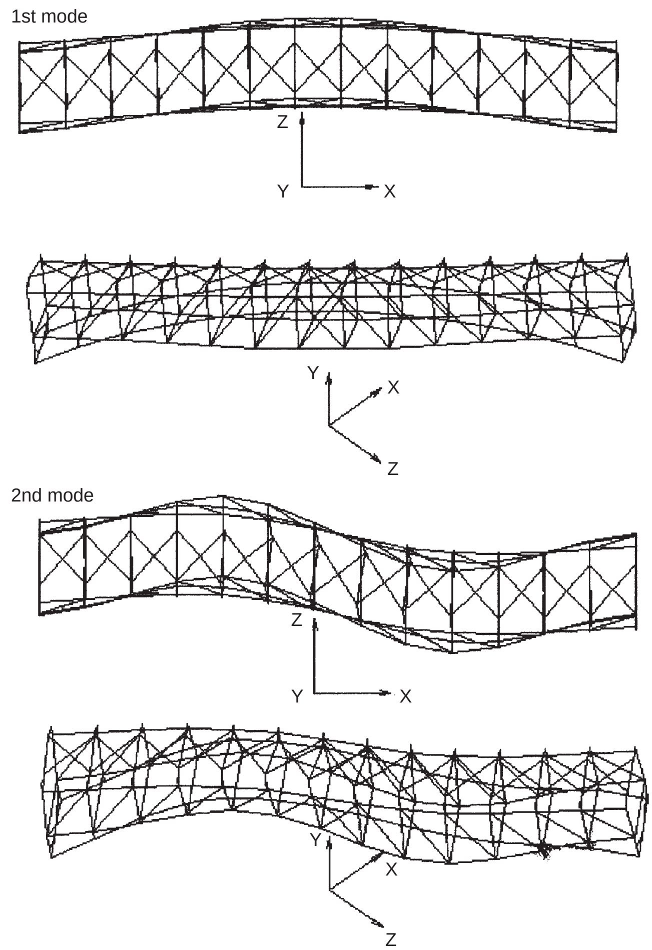

Fig. 4. Mode shapes for the first and second modes.

Table 4
Modal analysis results

Mode No.	Frequency (Hz)	Mode-shape
1	0.975	$X < Y < Z$
2	2.113	$X < Y < Z$
3	2.279	$Z < X < Y$
4	2.284	$Z < X < Y$
5	2.290	$Z < X < Y$
6	2.298	$Z < X < Y$

Table 5
Displacements due to dead and seismic loads

Direction	Due to dead load in mm	Due to seismic load in mm
X	−0.035	0.009
Y	−10.54	3.815
Z	0.001	110.95

Table 6
Dead load and seismic load stresses

Member	Dead load stress	Seismic load	Combined in
T7	−1346.88	1852.65	3199.53
D3	−1956.15	1650.48	3606.63
V4	1097.10	261.30	1358.40
A1	−2042.40	6325.23	8367.63
B7	273.93	1249.59	1523.52
C3	−413.45	12325.10	12738.55
V1	−529.23	6672.30	7201.53

allowable stresses to determine the earthquake load at which failure of various members occurs. The total stresses in all members were within allowable limits for a peak acceleration of $A = 0.06$ and $A = 0.19$. A few upper cross beam members failed at $A = 0.25$. For $A = 0.35$, which is representative of a Mercalli VIII scale earthquake, the bridge would experience severe damage that is mostly confined to the top cross bracings and top cross beams. It is expected that loss of most of the top cross bracing and beam members would cause severe damage to the top wind-bracing system.

6. Conclusions

The analyses demonstrated that the bridge was designed and built for a high factor of safety, since the design was based on controlled deflections [1]. Even though the bridge was built long ago, it is clear that the trusses can accommodate current AASHTO truck loadings provided the lower-chord joints that have severely deteriorated are properly repaired.

Seismic analysis showed that the restored bridge can withstand an earthquake of intensity VII modified Mercalli scale with acceleration coefficient $A = 0.19$. Certain bridge members failed for $A = 0.25$. However, their failure would only cause localized damage that would allow the bridge to function after the earthquake. For the highest effective peak acceleration examined in this system, i.e., $A = 0.35$, the bridge would be severely damaged. Given the fact that there are several hundred timber bridges in the eastern United States and that, according to historic data, they could experience higher than Mercalli VII earthquakes, a comprehensive and validated study including their seismic behavior is necessary. Since several of the bridges are in poor physical condition, considerable construction savings can be achieved by performing nonseismic and seismic rehabilitation work simultaneously. The effects of soil-structure interaction could also be of some concern and could be studied, provided geotechnical data is available, using well established rigorous and approximate procedures [12,13].

Acknowledgements

The authors would like to acknowledge the financial support of the West Virginia Department of Transportation, the National Science Foundation, and the Federal Highway Administration.

References

[1] Kemp EL, Hall J. Case study of burr truss covered bridge. Engrg Issues J Professional Activities, ASCE, 101 E13, 391-412 July, Proc. paper 11461, 1975.
[2] Cohen S. West Virginia covered bridges. Charleston, WV: Pictorial Histories Publishing Co., 1992.
[3] Standard Specifications for Highway Bridges, 15th Edition., AASHTO. Washington, DC: American Association of State Highway and Transportation Officials, 1992.
[4] TM5-809-10-1. Technical manual: seismic design guidelines for essential buildings. Washington, DC: Department of The Army, The Navy, and The Air Force, 1986.
[5] King HM, McColloch JS, Spyrakos CC. An earthquake hazard assessment for West Virginia, Final Report, West Virginia Geological and Economic Survey, December, 1993.
[6] Spyrakos CC. Finite element modeling in engineering practice. Pittsburgh, PA: Algor Publishing Division, 1996.
[7] Halabe UB, Rao Hota V. Nondestructive evaluation of wood using ultrasonic time and frequency domain analysis. Constructed Facilities Center, Final Report, West Virginia University, WV, 1993.
[8] Nondestructive Testing Handbook. Acoustic emission testing, American Society for Nondestructive Testing, vol. 5, 1987.
[9] Halabe UB, Gangarao HVS, Rao Hota V, Petro SH. Ultrasonic testing of Barrackville timber bridge, Report No. CFC-94-176, Constructed Facilities Center, West Virginia University, WV, 1994.
[10] Chen HL, Spyrakos CC, Venkatesh G. Evaluating structural deterioration by dynamic response. ASCE J Struct Division 1995;121(8):1197–204.
[11] Moody RC, Hernandez R, Davalos JF, Sonti SS. Yellow poplar glulam timber beam performance, USDA Forest Service Research Paper FPL-RP-520. Madison, WI: US Forest Products Laboratory, 1993:28.
[12] Spyrakos CC. Assessment of SSI on the longitudinal seismic response of short span bridges. Engrg Struct 1990;12:60–6.
[13] Spyrakos CC. Seismic behavior of bridge piers including soil-structure interaction. Comput and Struct 1992;43(2):373–84.